

A Comparative Study of Knowledge Transfer Methods for Misaligned Urban Building Labels

Bipul Neupane^{a,b,*}, Jagannath Aryal^{a,b}, Abbas Rajabifard^b

^a*Earth Observation and AI Research Group, Faculty of Engineering and IT, The University of Melbourne, Parkville, Melbourne, 3010, VIC, Australia*

^b*Department of Infrastructure Engineering, Faculty of Engineering and IT, The University of Melbourne, Parkville, Melbourne, 3010, VIC, Australia*

Abstract

Misalignment in Earth observation (EO) images and building labels impact the training of accurate convolutional neural networks (CNNs) for semantic segmentation of building footprints. Recently, three Teacher-Student knowledge transfer methods have been introduced to address this issue: supervised domain adaptation (SDA), knowledge distillation (KD), and deep mutual learning (DML). However, these methods are merely studied for different urban buildings (low-rise, mid-rise, high-rise, and skyscrapers), where misalignment increases with building height and spatial resolution. In this study, we present a workflow for the systematic comparative study of the three methods. The workflow first identifies the best (with the highest evaluation scores) hyperparameters, lightweight CNNs for the Student (among 43 CNNs from Computer Vision), and encoder-decoder networks (EDNs) for both Teachers and Students. Secondly, three building footprint datasets are developed to train and evaluate the identified Teachers and Students in the three transfer methods. The results show that U-Net with VGG19 (U-VGG19) is the best Teacher, and U-EfficientNetv2B3 and U-EfficientNet-lite0 are among the best Students. With these Teacher-Student pairs, SDA could yield upto 0.943, 0.868, 0.912, and 0.697 F1 scores in the low-rise, mid-rise, high-rise, and skyscrapers respectively. KD and DML provide model compression of upto 82%, despite marginal loss in performance. This new comparison concludes that SDA is the most effective method to address the misalignment problem, while KD and DML can efficiently compress network size without significant loss in performance. The 158 experiments and datasets developed in this study will be valuable to minimise the misaligned labels.

Keywords: building footprint extraction, collaborative learning, convolutional neural networks, semantic segmentation, transfer learning

1. Introduction

Extracting complex urban building footprints and roofs poses a significant challenge, demanding precise deep learning (DL)-based semantic segmentation methods. These methods rely on training CNN configurations like EDNs on very high-resolution (VHR) Earth observation (EO) images, precisely labelled for accuracy [1]. VHR image-label pairs are commonly sourced from airborne sensors and are manually annotated. Integration of APIs and secondary labels streamlines the creation of training data for an end-to-end DL training workflow [2]. The key challenge in this process comes from the off-nadir angles of airborne sensors, resulting in a misalignment between the images and building labels. The misalignment increases along with spatial resolution and building height, leading to reduced precision of high-rise urban building extraction, as depicted in Figure 1.

Recently, knowledge transfer methods have shown promise in addressing the misaligned building labels in off-nadir images [3]. In particular, the transfer learning method of SDA [4], and model compression methods such as KD [5] and DML [6] have

recently been introduced to address this problem. However, several critical questions remain unanswered regarding the influence of (i) a diverse collection of EDN configurations that are abundant in the computer vision domain, (ii) building height, and (iii) spatial resolution of EO images, for the effective implementation of these methods. Furthermore, there is a notable absence of diverse, error-free building footprint/roof datasets encompassing various building types, including high-rises and skyscrapers. In response to these challenges, this study presents a systematic workflow for method comparison and introduces new building datasets for the two-step training of knowledge transfer methods.

1.1. EDNs for building extraction

EDNs are defacto DL configurations for semantic segmentation of features including buildings as they allow the plug-and-play of modern CNNs and Transformers [7] as encoders. CNNs such as ResNet [8], VGGNet [9], DenseNet [10], etc. have long supported the task of semantic segmentation as a fundamental backbone for feature extraction from images. The early use of CNNs functioned for patch-based building extraction [11] with fully connected layers for classification. Later, these baseline CNN architectures were supported by the fully convolutional network (FCN) [12] configuration that replaced the fully connected layers with convolution operations to upsample and out-

*Corresponding author

Email addresses: bneupane@student.unimelb.edu.au (Bipul Neupane), jagannath.aryal@unimelb.edu.au (Jagannath Aryal)



Figure 1: Misalignment of building labels with an increase in spatial resolution and height of the building. The numbers in the labels show the height of the building and the red line shows the displacement of labels. The images are collected from *Nearmap Tile API* over the City of Melbourne, Australia.

put spatial maps instead of classification scores for pixel-level segmentation. EDN configurations such as U-Net [13] further replaced those final upsampling layers with a decoder unit to generate precise spatial maps and used the CNNs as the backbone (aka. encoder) for feature extraction. U-Net provided an effective trade-off between the use of context and precise localisation with “skip connections” in its EDN configuration. Its successors like ResUNet [14], U-Net++ [15], and U-Net3+ [16] densified the skip connections with residual connections, dense nested skip connections, and full-scale skip connections respectively. The overall aim was to improve the precision of the final segmented output by exploiting the multi-scale feature information to preserve both local and global context information. Unlike the U-Net, LinkNet [17] utilised “addition” operations instead of the increased use of “concatenation” to aggregate the feature maps transported by the skip connections. Distinctly, pyramid scene parsing network (PSPNet) [18] used a pyramid pooling module to focus on preserving the global context information in the images. Similarly, feature pyramid networks (FPNs) [19] captured multi-scale features with bottom-top and top-bottom pyramid structures. DeepLabv3+ [20] introduced atrous convolutions (aka. dilated convolution) with different dilation rates in parallel, to capture multi-resolution feature maps. Self-attention mechanism was introduced in the multi-attention network (MANet) [21] to dynamically fuse local features with their broader global dependencies. These EDNs have become instrumental in the precise segmentation of buildings, especially for low-rise rural buildings. However, urban buildings

carry additional challenges.

1.2. The misalignment problem and methods of restoration

Urban buildings are challenging to extract due to their complexity and the misalignment of buildings and labels due to off-nadir source imagery. Such challenges bring omission and registration noise to the building labels that are fundamental to training the EDNs. Several methods have been introduced to address the problem of misalignment in the training data of EDN-based semantic segmentation networks. Especially with the challenge of developing large error-free training data, approaches have been made to make the DL networks capable of learning from the noisy data. Two-step training of the networks – first on a large noisy dataset and secondly on a small error-free clean data – have become pivotal in increasing the network’s noise tolerance. Unlike training a network directly on the small clean data that leads to over-fitting [22], Mnih and Hinton [23] introduced this two-step training approach with a labelled noise model for a neural network to extract buildings from aerial images. Merely adapted for the misaligned building labels from aerial images, this is a common training approach in computer vision. Xiao et al. [24] introduced an intricately detailed noise model to describe the intricate relationship between images, noise labels, actual labels, and noise types in the context of image classification. Studies have also added additional top layers on their CNN to capture the relationship between clean and noisy labels [25, 26]. In aerial imagery, Maggiori et al. [27] pre-trained an FCN on noisy labels from GIS and fine-

tuned it on small clean data. This two-step training is a transfer learning method called supervised domain adaptation (SDA). Neupane et al. [4] use SDA to adapt an EDN between the building datasets of two spatial resolutions. Similarly, Xu et al. [3] employed knowledge distillation (KD) between a large and a small network trained on noisy and clean building data respectively. KD was initially developed by Hinton et al. [5] to distil the knowledge from an immovably large DL network (Teacher) into a smaller practically deployable network (Student), reducing the network parameters in the transfer stage. Xu et al. [3] use this concept to train a Teacher network on the large noisy data and distil a Student using a limited set of clean data. In this two-step training, the Teacher serves as a guide, enabling the Student to tap into its knowledge for noise-tolerant learning. The concept of KD was extended to deep mutual learning (DML) by Zhang et al. [6], which allowed an ensemble of Students to learn collaboratively and teach each other throughout the distillation.

1.3. Research questions and contributions

SDA, KD, and DML have been introduced to the problem of misaligned labels, however, several research questions are yet to be answered. A concrete conclusion is lacking on whether they are robust in addressing the misalignment problem in different building types. Furthermore, with the availability of multiple CNNs and EDNs for semantic segmentation, they have not been benchmarked to serve as the optimal Teacher (large immovable networks) and Student (lightweight and deployable) networks. This paper is therefore focused on answering the following research questions (**RQs**):

RQ1. What lightweight CNNs and hyperparameters in the EDNs provide efficiency gain in Teacher and Student networks of knowledge transfer methods?

RQ2. Are SDA and model compression techniques such as KD and DML effective in minimising the effects of misaligned building labels?

RQ3. How do SDA, KD, and DML perform on different building heights and spatial resolutions of EO images?

Answering the RQs requires a systematic experimental design with datasets to train the Teacher and Student networks. Further, training the EDNs in a Teacher-Student setting for the problem of misalignment requires a pair of noisy and clean building datasets. Therefore, the existing benchmark datasets such as Massachusetts Building dataset [28], WHU Building dataset [29], Inria Aerial Image Labeling dataset [30], Aerial Imagery for Roof Segmentation (AIRS) [31], xBD dataset [32], and SpaceNet Building dataset [33] are not able to facilitate our experimental settings. Additionally, the image-label pairs of cleanly labelled building datasets are not openly available as the existing datasets are not error-free [1]. To this end, we develop our own set of datasets including both large-and-noisy and clean datasets. We consider the main contributions of this study as follows:

- We extensively compare SDA, KD, and DML to generalise the buildings from complex urban settings, minimising the effects of misaligned labels due to off-nadir EO images.

Furthermore, we present a qualitative study of SDA, KD, and DML in four different building types: low-rise, mid-rise, high-rise, and skyscrapers.

- We develop a multi-resolution dataset for Teacher networks, a multi-resolution clean dataset for Student networks, and an evaluation dataset to evaluate the Teachers and Students. The Teacher’s dataset was developed in our previous study of [2]. The Student’s and evaluation datasets are newly developed with manually prepared labels on the image tiles that are collected from *Nearmap API service*. The developed datasets comprise complex urban buildings including high-rise and skyscraper buildings.
- We present an extensive hyperparameter search using a recent mobile CNN called MobileOne from Apple [34] in combination with different EDNs. The hyperparameter search includes five optimisers and nine loss functions. We further benchmark 43 mobile CNNs with network parameters lower than 20 million when integrated into the best-performing EDN from the hyperparameter search. The CNNs include EfficientNetv2 from Google [35], FBNet from Facebook and Berkeley [36], MobileViT transformer CNN from Apple [37] and other lightweight networks like MNASNet [38], and Huawei’s TinyNet [39]. To the best of our knowledge, such extensive benchmarking of lightweight CNNs and some of their integration into an EDN configuration is being performed for the first time for building extraction.

2. Materials and methods

The comparative study of the knowledge transfer methods is constructed with a carefully designed workflow to accommodate preliminary studies, development of datasets, and training of the best Teacher and Student networks as illustrated in Figure 2. First, we begin with the preliminary search of hyperparameters, followed by the search of CNN backbones and EDN architectures to mimic the Teacher and Student networks. The preliminary search is carried out on an existing benchmark dataset to show the robustness and reliability of the EDN architecture that we use in our study. Secondly, we develop the noisy and clean datasets necessary to study the knowledge transfer methods. Finally, we train and evaluate the methods on the prepared datasets.

2.1. Datasets

We use four datasets in this study including one benchmark dataset and three datasets that we prepare in this paper. The benchmark dataset is used for the preliminary investigation to find the hyperparameters, CNNs and EDNs for the Teacher and Student networks. The three other datasets are dedicated to knowledge transfer purposes.

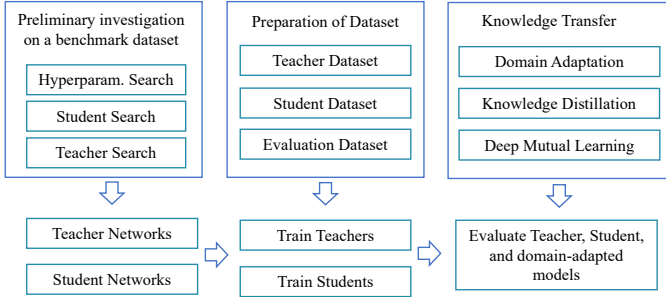


Figure 2: Research workflow designed to facilitate our systematic comparative study of the knowledge transfer methods.

- **Benchmark dataset:** We use the Massachusetts Building dataset [28] as a benchmark dataset for preliminary studies. It is one of the most used datasets for building extraction with DL due to its early release. For experimental consistency and to keep memory usage low, we use the smaller subset of the dataset that we used in our previous work [40]. In this subset, the original 1500x1500 tiles are split into 256x256 tiles and the total number of training and test images are reduced by 4x and 2x to reduce the computational time for our extensive comparison. The number of validation images is kept the same as in the original dataset. In total, the proportion of train-test-validation images is 800-160-100.
- **Teacher’s dataset (T)** is collected from our previous work [2]. The labels are developed by masking and tiling the building roof samples provided by the City of Melbourne. Multi-resolution images of 0.3, 0.6, and 1.2m spatial resolution are collected using *Nearmap Tile API*. The API provides easy and automated access to geo-referenced image tiles of 256x256 pixels. The images are not precisely orthorectified, causing a misalignment between the roof and footprint labels. This dataset serves as a Teacher’s dataset because of the unaccounted misalignment of labels. In total, 6626 train tiles and 643 validation tiles were produced in this dataset.
- **Student’s dataset (S)** is prepared by collecting image tiles of the central business district (CBD) of Melbourne, from *Nearmap Tile API* and orthorectified images of the same area. The CBD consists of mostly high-rise and skyscraper buildings with complex structures, adding to the problem of misaligned labels. The buildings are manually labelled over the image tiles, and the City of Melbourne’s building roof samples are overlaid over the orthorectified product. A total of 746 train tiles and 243 validation tiles were produced for this dataset.
- **Evaluation dataset (Ev)** is curated as a validation dataset, without training data to evaluate the knowledge transfer on the manually prepared ground truths (GTs). A subset of 55 image tiles of T is taken and manually annotated. Ev includes four types of buildings: low-rise, mid-rise, high-rise, and skyscrapers. The building types are

separated according to their heights as suggested by the Australian Bureau of Statistics. The (i) low-rise (1 to 3 storeys), mid-rise (4 to 8 storeys), and high-rise (9 to 19 storeys). Different from the super high-rises (more than 20 storeys), the height definition of skyscrapers is lacking in Australia. Therefore we assume a height of more than 150m as skyscrapers, similar to the other countries.

In summary, (i) T contains misaligned images and labels on both training and validation samples, (ii) S contains off-nadir images with manually annotated labels and orthorectified images with aligned labels of complex high-rise buildings, (iii) Ev contains off-nadir images of high-rise buildings from T and manually annotated samples. Samples of the T, S, and Ev datasets are shown in Figure 3.



Figure 3: Image and labels in the samples of the Teacher’s dataset (T), Student’s dataset (S), and Evaluation dataset (Ev).

2.2. Preliminary Investigation

A preliminary investigation is carried out to search for hyperparameters, CNNs, and EDNs for the Teacher and Student networks. The hyperparameters and CNNs are fundamental to achieving the highest evaluation scores in the semantic segmentation of buildings. A general EDN architecture is shown in Figure 4.

2.2.1. Hyperparameter search

Hyperparameter tuning is the most important preliminary step to achieve the highest evaluation scores out of any DL network. During this step, different hyperparameters are experimented such as the learning rate, batch size, converging epoch, loss functions, and optimisers. We experiment with five popular optimiser algorithms and nine loss functions. A scheduler is deployed with the optimisers to optimise the learning rate. A

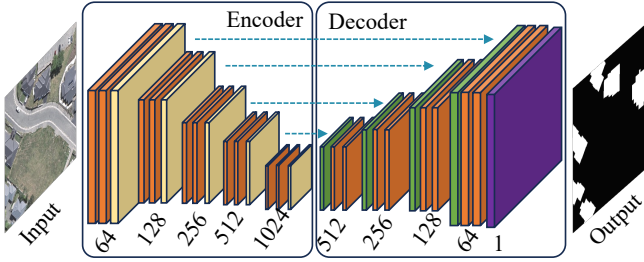


Figure 4: Network configuration of an EDN. The encoder (CNN) extracts multi-scale features using convolution and pooling operations. The decoder upsamples the feature maps collected from the bottleneck of CNN to output the final segmented map. Skip connections (dotted lines) are often used to transport the feature maps from the encoder layers to be utilised (concatenate/add) in the corresponding decoder layers.

CNN encoder is randomly selected and integrated into U-Net EDN for this search. The batch size is not investigated as it did not play a vital role in the benchmarking of Bakirman et al. [1] and our previous work. The networks are saved at the converging epoch.

2.2.2. EDNs for Teacher and Student

State-of-the-art EDNs of U-Net, U-Net++, U-Net3+, LinkNet, PSPNet, FPN, DeepLabv3+, and MANet are used as potential architectures for the Teacher and Student networks because of their popularity of semantic segmentation of EO images.

- i. *U-Net* [13] is an architecture characterised by its symmetrical structure, consisting of an encoder CNN and a decoder equipped with corresponding upsampling layers. This symmetrical design is implemented to effectively retain and preserve spatial information throughout the network. It leverages skip connections to transfer and concatenate low-level features from the encoder to the corresponding decoder layers with matching dimensions. Each encoder block consists of convolutions, Rectified Linear Unit (ReLU) and max pooling layers. Similarly, the decoder blocks consist of upsampling, concatenation and convolution operations. The encoder can be replaced by other CNNs.
- ii. *U-Net++* [15] is a reiteration of U-Net with nested dense skip connections that enrich the information transported to the decoder layers and reduce the inter-encoder-decoder semantic gaps. The encoder and decoder blocks are similar to the U-Net, however, the skip connections have additional convolution layers.
- iii. *U-Net3+* [16] is the latest reiteration of the U-Net family. Once again, its focus is on improving the skip connections. It offers a full-scale skip connection to reduce the inter-encoder-decoder and intra-decoder semantic gaps. Its decoder layer receives the feature maps of (i) the same-scale encoder layer, (ii) smaller-scale encoder layers supported by non-overlapping max pooling operations, and (iii) larger-scale decoder layers supported by bilinear interpolation. All incoming feature maps are unified with

64 filters of 3x3 size. Subsequently, a feature aggregation mechanism is employed on these 320 (64×5) concatenated maps of five scales. This unification reduces the number of network parameters compared to both U-Net and U-Net++, however, it takes more time to compute because of the increased concatenation operations.

- iv. *LinkNet* [17] has a similar architecture to U-Net, except the features transported by skip connections are added to the decoder layers. The input of the encoder layer is bypassed to the output of the decoder layer with matching dimensions. This recovers the spatial information lost in down-sampling and further reduces the network parameters. The original LinkNet uses ResNet-18 CNN as its encoder, but it can be replaced by others.
- v. *PSPNet* [18] is different from the symmetrical EDNs above. A CNN is used to collect the feature maps that are then input to a pyramid pooling module (PPM). PPM extracts multi-scale contextual information from the features by dividing them into cells, performing pooling operations within each cell to capture features at different scales, and then concatenating these results. This enriched information is integrated into the network’s decoder, improving the accuracy of semantic image segmentation by considering details and context at various levels of scale.
- vi. *FPN* [19] captures multi-scale features with bottom-top and top-bottom pyramid structures. The bottom-top pathway enhances feature maps obtained from a CNN by applying lateral connections, facilitating information propagation from lower-resolution to higher-resolution feature maps. The top-bottom pathway upsamples higher-level feature maps and fuses them with the bottom-up feature maps. This fusion creates a multi-scale feature pyramid, offering semantically rich and precisely localised information at various resolutions. FPN’s feature pyramid enables effective handling of objects of different sizes within images. Originally dedicated to object detection, it is useful to segment objects of different sizes with precise boundary extraction.
- vii. *DeepLabv3+* [20] is the latest reiteration of the DeepLab family. The encoder comprises a CNN responsible for gathering high-level features from the input image. To capture multi-resolution feature maps, an atrous spatial pyramid pooling (ASPP) module is integrated into the encoder, utilizing atrous convolutions (also known as dilated convolutions) with different dilation rates in parallel. The results of these parallel convolutions are combined to create a holistic feature representation, preserving both local and global contextual information. In the decoder, feature maps from the encoder are upsampled using either bilinear interpolation or transposed convolutions.
- viii. *MANet* [21] uses a CNN to generate multi-scale hierarchical feature maps of different scales. The maps are then integrated (generally concatenated) into multiple attention heads, each dedicated to a single scale of feature maps. These attention heads operate in parallel, allowing the network to attend to various features simultaneously. Deconvolution layers upsample the outputs of attention heads

from the smallest to the input size feature maps to produce the final segmented output.

2.2.3. Encoders for Student

EDNs with the best trade-off between the network parameters (size) and the evaluation scores are selected to test the CNNs for Student networks. As the knowledge transfer methods that we are studying include model compression techniques, lightweight CNNs are chosen as the encoders of the EDNs to prepare the Student networks. We search for lightweight mobile CNNs that are well-recognised in the computer vision domain and those that can be integrated as an encoder within an EDN configuration for the segmentation of buildings. We identified 43 such CNNs from 16 families. Out of these, the ones with the highest evaluation scores, the smallest size, and the ones with the best trade-off between network parameters and evaluation scores are chosen as the Student networks. Only the CNNs with network parameters lower than 20 million, when integrated into U-Net, are studied as Students. The identified CNNs are:

- i. *ResNet* [8] is one of the earliest CNNs. Its success comes from the introduction of residual learning and skip connections into CNN that allowed the training of deeper models. They are either two-layers deep (ResNet-18, -34) or three-layers deep (ResNet - 50, -101, -152), with ResNet-18 as the lightest one.
- ii. *DenseNet* [10] employs dense blocks to establish dense connections between layers, enabling linkage of all the layers with matching feature-map sizes. DenseNet-121 is the lightest among DenseNet-121, -169, and -201, where the numbers denote the depth of the networks.
- iii. *MobileNet* [41] is a lightweight CNN designed for vision tasks on mobile and embedded devices, emphasizing low latency. It leverages depthwise separable convolutions for efficiency. Its iteration, MobileNet-v2 [42], introduces inverted residual blocks to its bottleneck to minimise network parameters. The third iteration, MobileNet-v3 [43], is fine-tuned for mobile phone CPUs using network architecture search (NAS) [44] and NetAdapt algorithms to achieve efficient design. Multiple versions of MobileNet-v3 are accessible, catering to diverse resource constraints, and offering both compact and more resource-intensive options.
- iv. *MnasNet* [38] is a CNN tailored specifically for mobile devices, discovered through automated mobile NAS. It incorporates model latency as its main objective to identify a model that achieves a balance between precision and latency. MnasNet relies on inverted residual blocks, originally hailing from MobileNet-v2, as its fundamental building blocks. MnasNet-small is the lightest version of it.
- v. *EfficientNet* [45] follows the structure of MnasNet, but with FLOPs (floating point operations per second) as the main rewarding parameter. This is the baseline for the EfficientNetB0, which is further scaled from B1 to B7 with added depth, width, and image resolution. EfficientNet-lite versions are dedicated to mobile devices with ReLU6 activation functions and removed squeeze-and-excitation blocks.
- vi. *SK-ResNet* is an upgrade to ResNet with Selective Kernel (SK) unit [46] replacing the large kernel convolutions in its bottleneck, and allowing adaptive selection of receptive field size. SK-ResNet-18 is its lightest version.
- vii. *Dual path network (DPN)* [47] blends ResNet’s feature re-usage capacity with DenseNet’s features exploration strategy, developing a new topology of internal connection paths. DPN-68 is its lightest version.
- viii. *ResNeSt* [48] applies channel-wise attention to different branches of ResNet to capture cross-feature interactions and learn diverse representations. ResNeSt-18 is its lightest version.
- ix. *GERNet* is the GPU-efficient network (GE-Net) [49] implementation on ResNet that allows a more inexpensive search for GPU-efficient networks compared to NAS. Available versions are small, medium, and large.
- x. *MobileOne* [34] from Apple is built upon Google’s MobileNet-v1 and MobileNet-v2, dedicated to its mobile devices. They achieved a 1 ms inference in iPhone-12 time by removing the multi-branched architecture during the inference. Five versions of it are available from smallest to largest.
- xi. *High-Resolution Net (HRNet)* [50] is a CNN focused on preserving high-resolution features throughout the network. HRNet-18 is its lightest version.
- xii. *MobileViT* [37] is a lightweight vision transformer with low latency from Apple dedicated to mobile devices. It offers an alternative approach to handling global information processing using transformers, namely, treating transformers as convolutional units. It comes with small versions ranging from s, xs, and xxs.
- xiii. *Facebook-Berkeley-Net (FBNet)* [36] is a mobile CNN discovered through automated mobile differentiable NAS. It employs an image block with depthwise convolutions and an inverted residual structure inspired by MobileNetv2.
- xiv. *HardCoRe-NAS* [51] is developed to address the “soft” enforcement of constraint by NAS. It employs a scalable search that adheres to hard constraints throughout the search and is based on an accurate definition of the anticipated resource requirement.
- xv. *MixNet* [52] is a mobile CNN from Google Brain that proposes mixed depthwise convolution (MixConv) that is capable of mixing multiple kernel sizes in a single convolution in MobileNets. Three versions of MixNet are available: small, medium, and large.
- xvi. *TinyNet* [39] is a mobile CNN from Huawei, that is inspired by the scalability of EfficientNet with three dimensions of depth, width, and image resolution. They summarise and derive several TinyNets from EfficientNetB0 based only on depth and image resolution. The size of TinyNet ranges from a to e .

The reiteration, EfficientNetv2 [35], later added Fused-MBConv convolutional blocks along with the NAS component. Similar to v1, several versions are scaled up for v2.

- The reiteration, EfficientNetv2 [35], later added Fused-MBConv convolutional blocks along with the NAS component. Similar to v1, several versions are scaled up for v2.
- vi. *SK-ResNet* is an upgrade to ResNet with Selective Kernel (SK) unit [46] replacing the large kernel convolutions in its bottleneck, and allowing adaptive selection of receptive field size. SK-ResNet-18 is its lightest version.
 - vii. *Dual path network (DPN)* [47] blends ResNet’s feature re-usage capacity with DenseNet’s features exploration strategy, developing a new topology of internal connection paths. DPN-68 is its lightest version.
 - viii. *ResNeSt* [48] applies channel-wise attention to different branches of ResNet to capture cross-feature interactions and learn diverse representations. ResNeSt-18 is its lightest version.
 - ix. *GERNet* is the GPU-efficient network (GE-Net) [49] implementation on ResNet that allows a more inexpensive search for GPU-efficient networks compared to NAS. Available versions are small, medium, and large.
 - x. *MobileOne* [34] from Apple is built upon Google’s MobileNet-v1 and MobileNet-v2, dedicated to its mobile devices. They achieved a 1 ms inference in iPhone-12 time by removing the multi-branched architecture during the inference. Five versions of it are available from smallest to largest.
 - xi. *High-Resolution Net (HRNet)* [50] is a CNN focused on preserving high-resolution features throughout the network. HRNet-18 is its lightest version.
 - xii. *MobileViT* [37] is a lightweight vision transformer with low latency from Apple dedicated to mobile devices. It offers an alternative approach to handling global information processing using transformers, namely, treating transformers as convolutional units. It comes with small versions ranging from s, xs, and xxs.
 - xiii. *Facebook-Berkeley-Net (FBNet)* [36] is a mobile CNN discovered through automated mobile differentiable NAS. It employs an image block with depthwise convolutions and an inverted residual structure inspired by MobileNetv2.
 - xiv. *HardCoRe-NAS* [51] is developed to address the “soft” enforcement of constraint by NAS. It employs a scalable search that adheres to hard constraints throughout the search and is based on an accurate definition of the anticipated resource requirement.
 - xv. *MixNet* [52] is a mobile CNN from Google Brain that proposes mixed depthwise convolution (MixConv) that is capable of mixing multiple kernel sizes in a single convolution in MobileNets. Three versions of MixNet are available: small, medium, and large.
 - xvi. *TinyNet* [39] is a mobile CNN from Huawei, that is inspired by the scalability of EfficientNet with three dimensions of depth, width, and image resolution. They summarise and derive several TinyNets from EfficientNetB0 based only on depth and image resolution. The size of TinyNet ranges from a to e .

2.2.4. Teacher Search

The Teacher network is based on the performance of the Student networks. The size of the networks is not taken as a measure to select a Teacher network as it is theoretically a large immovable network to distil from. The larger version of the CNNs selected as the Student can be used as the Teacher network. For example, if EfficientNetB0 is selected as the Student, one way to select the Teacher is to choose the largest network in the family of EfficientNet.

2.3. Knowledge transfer

Three knowledge transfer methods – SDA, KD, and DML – are studied to minimise the effects of misaligned labels. An illustrative example of the three knowledge transfer methods is shown in Figure 5. We explain each method in the next subsections.

2.3.1. Supervised Domain adaptation

SDA is a transfer learning method where samples are available in both the source and the target domain [53]. The idea is to adapt a DL model pre-trained in a source dataset to a different target dataset by executing one more level of training on the new dataset. The low-level features are reused and preserved by initialising the learnable parameters (weights) close to local minima as learned from the source data, while the high-level parameters are updated to adapt to the target data [54]. The datasets T and S serve as the source and target respectively in our case. The EDNs with different CNNs are pre-trained on T and domain adapted to S. An illustrative example of the process is shown in Figure 5(a).

2.3.2. Knowledge Distillation

KD, as introduced by Hinton et al. [5], is a technique for compressing knowledge from a large, complex model into a smaller, deployable model while minimising the loss in performance. In the context of cross-modal distillation, where a Teacher network is trained on noisy samples and a Student network on clean ones [3], we employ a similar approach of KD in our work. The Teacher is trained on the noise-unaccounted T dataset. It yields subpar building segmentation results in the presence of noisy label types but excels in the case of noise-lacking building types due to its exposure to a vast dataset. In contrast, the Student network is trained using the limited set of clean-labeled samples of S. This collaborative process empowers the Student network to overcome the challenges posed by noisy labels while also acquiring the ability to accurately extract buildings without mislabeling the classes found in the Teacher network. We utilise the EDN configuration that exhibits the best trade-off between size and evaluation scores as the Teacher. Then we explore various Student networks with lower network parameters (size) to achieve model compression. An illustrative example of KD with a Teacher and a Student of EDN configurations is depicted in Figure 5(b).

2.3.3. Deep Mutual Learning

DML [6] is a collaborative training technique where an ensemble of Student networks learn collaboratively from each other during training. Instead of relying solely on labelled data and a Teacher network, each Student’s loss function is ensemble to encourage agreement with the predictions of other Students. For simplicity, we ensemble the loss by taking the average loss among the number of Students. The goal is to achieve a consensus among the Students on correct predictions, enhancing model generalization and robustness. After training, the ensemble of Student networks can make more accurate predictions than individual networks. DML is valuable when dealing with limited labelled data such as our dataset S. An illustrative example of DML with a Teacher and two Students of EDN configurations is depicted in Figure 5(c).

2.4. Experimental Settings

2.4.1. Training parameters

Training parameters ensure re-producible methods. All DL networks are wrapped in the Pytorch framework using *python* library of *Segmentation Models Pytorch* [55]. The step/epoch is set as the ratio of the number of training images to the batch size of 2. The Teacher and Student networks are trained up to 50 and 200 epochs respectively. The learning rate is reduced upon a plateau of intersection over union (IoU) metric by a factor of 0.1 with patience of 10 epochs. A *sigmoid* function is used to obtain the final output maps for the binary segmentation of two classes “background” and “building”.

2.4.2. Evaluation measures

Four accuracy measures are used for evaluation in this work: precision (P), recall (R), IoU, and F1 score. P and R measure the accuracy of positive predictions made by the segmentation model, and the completeness of the segmentation results. IoU and F1 are calculated from the ‘area-of-overlap’ between prediction and binary labels and the ‘area-of-union’ (all of the predictions + binary labels - the overlap). The network with the highest F1 score is chosen as the network to study the knowledge transfer techniques. The mathematical notation of the four measures are

$$P = \frac{TP}{TP + FP} \quad (1)$$

$$R = 1 - \frac{TP}{TP + FN} \quad (2)$$

$$IoU = \frac{TP}{TP + FN + FP} \quad (3)$$

$$F1 \text{ score} = \frac{2 \times TP}{2 \times TP + FN + FP} \quad (4)$$

where, TP implies prediction = 1, label = 1; TN implies prediction = 0, label = 0; FP implies prediction = 1, label = 0; and FN implies prediction = 0, label = 1.

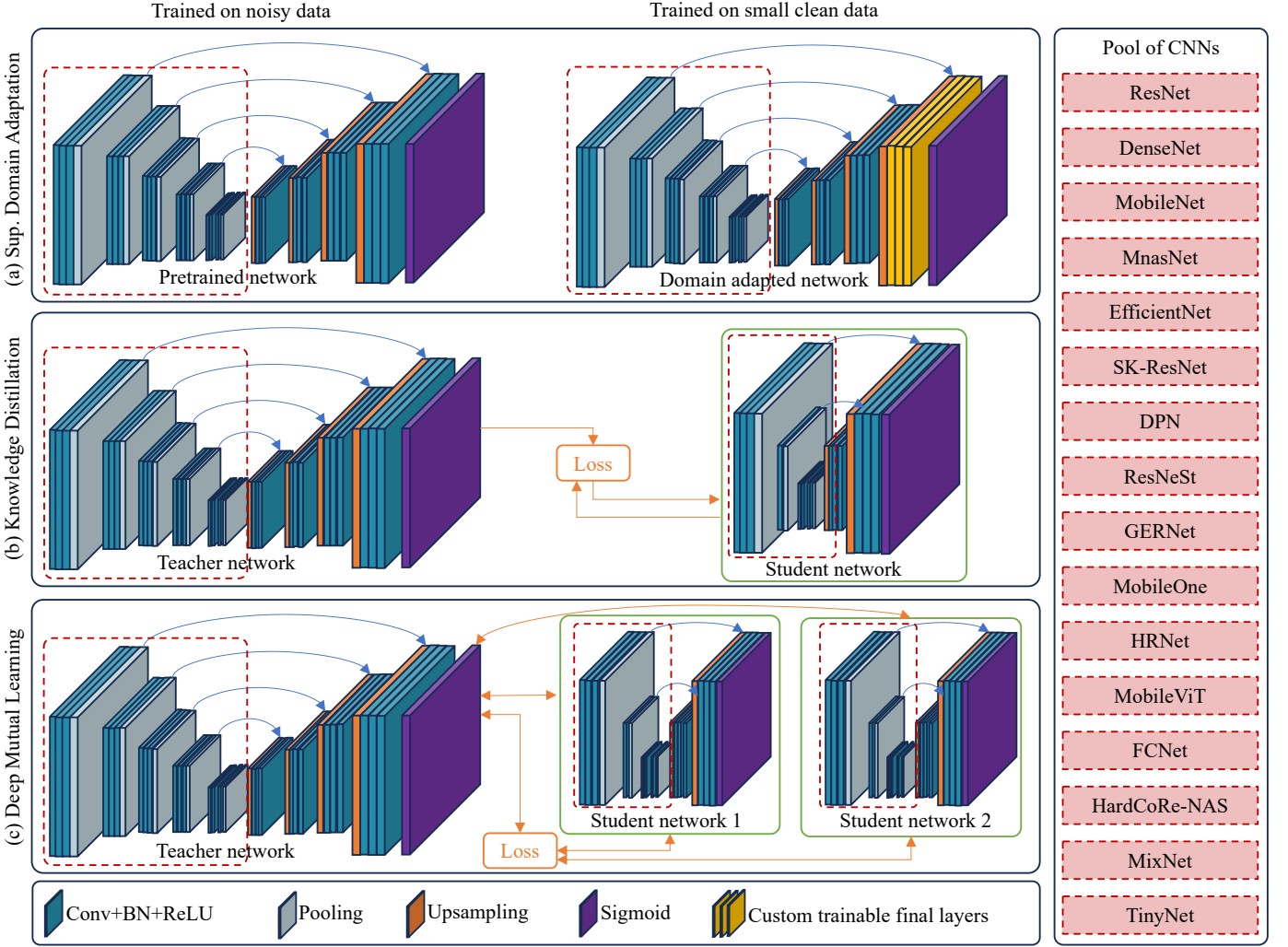


Figure 5: Illustrative example of the three knowledge transfer methods. (a) SDA of an EDN trained on noisy data and domain adaptation on small clean data. (b) KD of a Teacher network trained on noisy data to Student network distilled on a small clean data. (c) DML between one Teacher network trained on noisy data and two Student networks that are collaboratively distilled on the small clean data. The EDNs used in all methods can use the CNNs of different families from the Pool of CNNs as their encoder.

3. Results

The results are structured similarly to the workflow of Figure 2. A preliminary search of hyperparameters, CNNs and EDNs for the Student networks is presented first. The search uses the subset of the benchmark dataset as discussed earlier. Five Student networks are then selected from the preliminary search. The search is further carried out on the same dataset to find the best Teacher network. With the best EDN combination for the Teacher network and the five Student networks, the three knowledge transfer methods are further carried out on the T, S, and Ev datasets that we developed. A set of baseline scores is then generated without domain adaptation and distillation to compare the results produced by the three methods. The SDA, KD, and DML are then performed one by one.

3.1. Hyperparameter Search

Searching for the best hyperparameters results in the highest possible evaluation results from a DL network. To begin

this search, we randomly select MobileOne-s1 CNN as an encoder for a U-Net EDN, namely, U-MobileOne-s1. Then using the loss function of *total loss*, five optimisers including Adam, stochastic gradient descent (SGD), RMSprop, Adadelta, and Nadam are compared to find the optimiser that yields the highest evaluation scores. The *total loss* is formulated as the sum of *dice loss* and *binary focal loss*. The RMSProp optimiser yielded the highest scores for our experimental settings with a good trade-off between loss and faster-converging epoch. Then using RMSProp, nine loss functions – *binary cross entropy (BCE)*, *BCE dice loss*, *BCE Jaccard loss*, *binary focal dice loss*, *binary focal Jaccard loss*, *Jaccard loss*, *dice loss*, *binary focal loss*, and *total loss* – are further compared. A combination of RMSProp optimiser and *dice loss* yielded the highest scores as shown in Table 1. The results are similar to our benchmarking of larger CNNs in our previous work [40] and the comparison of Bakirman et al. [1]. Adam is marginally close to RMSProp optimiser. *Jaccard loss* produces the same IoU and F1 scores

with a faster-converging epoch compared to *dice loss* but yields a lower loss value on the validation set of the dataset used. In most of the experiments, the rate of 0.0001 produced the highest scores.

Table 1: Hyperparameter search using a U-Net with randomly chosen mobile CNN of MobileOne-s1. Five optimisers are tested with a Total loss (Dice loss + binary focal loss). The optimiser with the highest F1 score is then used to test the nine loss functions. The training time is reported with millisecond/iteration (ms/it) and the converging epoch is reported by Ep. The highest scores are highlighted in bold.

	Loss	P	R	IoU	F1	ms/it	Ep.
Optimisers (with Total Loss)							
Adam	0.177	0.959	0.963	0.926	0.960	376	26
SGD	0.338	0.889	0.990	0.882	0.935	200	28
RMSProp	0.177	0.958	0.964	0.927	0.961	294	22
Adadelta	0.444	0.927	0.784	0.744	0.845	420	29
Nadam	0.179	0.957	0.965	0.927	0.961	395	20
Loss Functions (with RMSProp optimiser)							
BCE	0.200	0.950	0.973	0.927	0.961	658	26
BCE Dice	0.243	0.949	0.975	0.928	0.961	658	15
BCE Jaccard	0.285	0.946	0.978	0.927	0.961	312	14
Binary Focal Dice	0.191	0.951	0.966	0.922	0.958	324	7
Binary Focal Jaccard	0.217	0.955	0.967	0.926	0.960	292	26
Jaccard	0.072	0.953	0.972	0.928	0.962	282	18
Dice	0.039	0.948	0.977	0.928	0.962	314	20
Binary Focal	0.120	0.975	0.896	0.876	0.932	292	30
Total Loss	0.177	0.958	0.964	0.927	0.961	294	22

The hyperparameter search leads to the *dice loss* as the primary loss function, which can be defined as:

$$L_{dice} = 1 - \frac{2y_j p_j + 1}{y_j + p_j + 1} \quad (5)$$

where y_j and p_j represent the GT and prediction respectively. The smooth value of 1 is added in the numerator and denominator to make sure that the function is defined in the case of $y_j = p_j = 0$, which is called an edge case scenario. The product of y_j and p_j represents the intersection between the GT and prediction.

In KD and DML, the *dice loss* of GT and prediction is not enough to quantify the differences between Teacher and Student networks. Therefore, to facilitate a student loss, we set up the weighted sum of the Student’s *dice loss* and a *distillation loss*. A *distillation loss* is employed to generalise the performance of the Student during KD and DML. This loss effectively reduces the differences in multi-scale feature maps between the Teacher and Student networks. The total weighted loss is denoted as:

$$L_{total} = \alpha L_{dice} + (1 - \alpha) L_{distil} \quad (6)$$

where α determines the weight assigned to the student loss, while $1 - \alpha$ determines the weight assigned to the distillation loss (L_{distil}). By adjusting the value of α , one can control the trade-off between optimising the Student’s performance on the actual task (student loss) and having it mimic the Teacher’s soft predictions (L_{distil}) which is formulated as:

$$L_{distil} = L_{MSE} \left(\sigma(p_j^t / T), \sigma(p_j^s / T) \right) \quad (7)$$

where p_j^t and p_j^s denote the prediction respectively from Teacher and Student networks for j^{th} pixel, σ represents the *sigmoid* activation function, T is temperature, and L_{MSE} is Mean Square Error Loss described in Eqn. 8. The *sigmoid* function takes the logits (raw scores) produced by the networks and converts them into probability values that sum to 1. T is introduced to modify the *sigmoid* function. It’s a positive scalar hyperparameter that controls the “softness” or “sharpness” of the probability distribution. T is typically set to a value greater than 1. A higher T softens the distribution, spreading probabilities more evenly among classes, and encouraging exploration. A lower T sharpens the distribution, emphasizing the most likely classes for more focused predictions. Adjusting T helps control the trade-off between exploration and confidence during knowledge transfer, allowing fine-tuning for specific tasks and datasets. In other words, T can be used to define a degree of freedom for the student that can be used to explore new ways of generalisation.

The original work of DML [6] uses the Kullback-Leibler (KL) Divergence Loss to measure the dissimilarity between probability distributions. In KD, it encourages the Student network to match the soft predictions (probability distribution) of the Teacher network. It is more applicable if the Teacher produces soft predictions with well-calibrated probabilities. Our experimental results show that the Teacher produces soft predictions that are not well-calibrated. In other words, our primary aim is to calibrate the building labels onto the roofs of the buildings. Therefore, to shift the objective from matching probability distribution to directly matching the predictions, we use the MSE Loss denoted as:

$$L_{MSE} = \frac{1}{N} \sum_{i=1}^N (y_j - p_j)^2 \quad (8)$$

where y_j and p_j respectively denote the GT and prediction for j^{th} pixel, $\frac{1}{N}$ is the normalisation factor used to compute the average squared difference.

3.2. Student Search

With the best hyperparameters found, we further use the U-MobileOne-s1 network with RMSProp optimiser and *dice loss* to compare seven other EDNs similar to U-Net. This includes U-Net, DeepLabv3+, LinkNet, MANet, U-Net++, and PSPNet. Due to the unavailability of the combination U-Net3+ and MobileOne-s1 in Keras and PyTorch frameworks, we are unable to present the results for the Student search. The results are shown in the first half of Table 2.

Results show that the U-Net++ yields the highest evaluation scores. However, the U-Net is marginally close to U-Net++ and it offers faster training and lower network parameters. On top, U-Net has less complexity because of its plain skip connections, allowing easy integration of recent complex CNNs into its network configuration. Therefore, trading off the marginally higher evaluation scores with lower parameters and faster training time, which are necessary to produce the small deployable Student networks, we use U-Net to search for lightweight CNNs for the Student networks. MANet produced IoU and F1

Table 2: Search of EDN and CNN encoders for Student networks. Eight EDNs are first tested with a randomly chosen MobileOne-s1 CNN to identify the EDN with the best trade-off between network parameters and evaluation scores. The highest scores among the EDNs are highlighted in bold. This EDN is then used to test and benchmark the 43 identified lightweight CNNs. Network parameters (Par.) are shown in Millions. The top 3 scores for the lightweight CNNs are underlined and ranked in order from 1 to 3 with a postscript. In addition to the lightweight CNNs, we also added VGG-19 CNN into this table, which was the highest scorer from our previous work [40].

	Par.	Loss	P	R	<u>IoU</u>	F1	ms/it
EDN with MobileOne-s1 encoder							
U-Net	9.1	0.039	0.948	0.977	0.928	0.962	314
DeepLabv3+	5.7	0.044	0.937	0.979	0.919	0.956	287
LinkNet	6.2	0.042	0.945	0.973	0.922	0.958	326
MANet	53.3	0.039	0.948	0.976	0.928	0.961	376
U-Net++	12.3	0.036	0.954	0.975	0.933	0.964	395
FPN	5.7	0.062	0.887	1.000	0.887	0.938	309
PSPNet	3.8	0.062	0.887	1.000	0.887	0.938	168
U-Net (best trade-off of Par. and F1) with lightweight CNNs as encoder							
ResNet-18	14.3	0.038	0.949	<u>0.977</u> ³	0.929	0.962	109
DenseNet-121	13.6	<u>0.037</u> ³	0.950	<u>0.977</u> ³	<u>0.931</u> ³	<u>0.963</u> ³	629
SE-ResNet-18	14.4	0.039	0.950	0.974	0.927	0.961	<u>151</u> ¹
MobileNet-v2	6.6	0.039	0.951	0.972	0.927	0.961	201
MobileNetv3-s	3.6	0.044	0.940	0.974	0.918	0.956	281
MobileNetv3-l	6.7	0.043	0.946	0.970	0.921	0.957	316
Eff.NetB0	6.3	0.038	<u>0.952</u> ³	0.973	0.929	0.962	304
Eff.NetB1	8.8	0.038	<u>0.950</u>	0.976	0.930	0.962	461
Eff.NetB2	10.0	<u>0.037</u> ³	<u>0.956</u> ¹	0.971	<u>0.931</u> ³	<u>0.963</u> ³	459
Eff.NetB3	13.2	<u>0.037</u> ³	0.951	<u>0.977</u> ³	0.930	<u>0.963</u> ³	485
Eff.Net-lite0	5.6	0.039	0.950	0.974	0.928	0.962	187
Eff.Net-lite1	6.4	0.039	0.948	0.976	0.928	0.961	233
Eff.Net-lite2	7.2	0.039	0.948	0.975	0.927	0.961	229
Eff.Net-lite3	9.4	0.038	0.948	<u>0.978</u> ²	0.929	0.962	258
Eff.Net-lite4	14.4	0.040	0.945	<u>0.978</u> ²	0.926	0.960	313
Eff.Netv2B0	7.6	0.038	0.951	0.975	0.929	0.962	284
Eff.Netv2B1	8.6	<u>0.037</u> ³	<u>0.953</u> ²	0.975	<u>0.931</u> ³	<u>0.963</u> ³	334
Eff.Netv2B2	10.4	<u>0.037</u> ³	0.951	<u>0.977</u> ³	<u>0.931</u> ³	<u>0.963</u> ³	347
Eff.Netv2B3	14.6	<u>0.035</u> ¹	<u>0.956</u> ¹	0.975	<u>0.934</u> ¹	<u>0.965</u> ¹	408
SK-ResNet-18	14.6	0.038	0.948	<u>0.978</u> ²	0.929	0.962	201
DPN-68	17.0	0.041	0.945	0.975	0.924	0.959	493
ResNeSt-14	17.6	<u>0.036</u> ²	<u>0.952</u> ³	<u>0.977</u> ³	<u>0.932</u> ²	<u>0.964</u> ²	<u>159</u> ²
GERNet-s	12.8	0.040	0.947	0.974	0.925	0.960	<u>180</u> ³
MobileOne-s0	8.6	0.038	0.948	<u>0.979</u> ¹	0.930	0.963	610
MobileOne-s1	9.1	0.039	0.950	0.975	0.928	0.962	287
MobileOne-s2	13.6	0.039	0.949	0.975	0.928	0.961	296
MobileOne-s3	16.2	0.039	0.950	0.973	0.927	0.961	293
HRNet-18	16.1	0.038	<u>0.952</u> ³	0.974	0.929	0.962	870
MNASNet-s	<u>2.2</u> ¹	0.043	0.938	<u>0.978</u> ²	0.920	0.957	214
MobileViT-s	8.0	0.040	0.946	0.975	0.925	0.960	289
MobileViT-xs	4.3	0.040	0.947	0.975	0.926	0.960	294
MobileViT-xxs	<u>3.1</u> ³	0.042	0.943	0.975	0.922	0.958	299
FBNet-c100	<u>5.2</u>	0.041	0.947	0.973	0.924	0.959	229
FBNet-v3b	8.6	0.042	0.943	0.974	0.921	0.958	690
FBNet-v3d	10.3	0.041	0.943	<u>0.978</u> ²	0.925	0.960	769
FBNet-v3g	16.8	0.040	0.945	0.976	0.925	0.960	917
HardCoRe-NAS-a	6.5	0.042	0.940	<u>0.979</u> ¹	0.922	0.958	283
HardCoRe-NAS-f	9.4	0.043	0.937	0.980	0.920	0.957	552
MixNet-s	4.3	0.044	0.943	0.970	0.918	0.956	429
MixNet-m	5.2	0.043	0.943	0.974	0.921	0.957	498
MixNet-l	7.6	0.041	0.948	0.972	0.924	0.959	532
TinyNet-a	6.7	0.042	0.944	0.975	0.923	0.959	296
TinyNet-e	<u>2.3</u> ²	0.045	0.934	<u>0.979</u> ¹	0.916	0.955	182
U-Net with VGG19 (not a lightweight CNN)							
VGG-19	29.1	0.033	0.962	0.974	0.939	0.967	223

similar to U-Net but with almost 6 times the network parameters. LinkNet and DeepLabv3+ are more lightweight than U-Net but yield lower scores. FPN and PSPNet which trained

faster, over-fit on the dataset.

The search for lightweight encoders for U-Net is shown in the second half of Table 2. We carefully integrate 43 such CNNs with network parameters lower than 20 million, into the U-Net configuration. The goal here is to select the top five Students for the comparative study of knowledge transfer. Among the 43 networks, the EfficientNetv2B3 yielded the highest IoU (0.934) and F1 (0.965) scores. The other high performers based on F1 score in order are ResNeSt-14, DenseNet-121, EfficientNetB2, and EfficientNetB3. The order is the same when comparing the least validation loss, and is similar when comparing the IoU scores. However, the purpose here is to find the lightweight CNNs. So keeping the highest scorer as one potential student, we search for other lightweight students. Interestingly, EfficientNet-lite0 shows the best trade-off between evaluation scores and network parameters, making it another potential student. For the remaining three students, the lightest networks with the lowest network parameters are chosen. The lightest ones are MNASNet-s, TinyNet-e, and MobileViT-xxs with 2.2, 2.3, and 3.1 Million network parameters respectively.

Apart from the lightweight networks, we also include the VGG-19 at the end of Table 2, which is the highest scorer from our previous work [40]. The purpose here is to show the marginal difference in its performance compared to EfficientNetv2B3. Furthermore, as we are taking U-VGG19 as one of the potential Teacher networks in the next step. Figure 6 shows the segmentation results of U-Net with VGG-19 and the selected five student networks on two randomly picked samples from the validation set of the Massachusetts building dataset. It is seen from the results that the network performance decreases with its size.

3.3. Teacher Search

The Teacher network is searched without any bound of the network parameters. From the previous results, U-EfficientNetv2B3 was the highest-performing Student network among the lightweight combinations. Therefore, we take the largest network of the same family as a potential Teacher network to mimic the “immovable large, difficult to deploy network”, which is EfficientNetv2L. As the Teacher network can be large and is not bounded by size, we also use U-Net with VGG-19 CNN as another potential Teacher for the experimental purpose. We compare eight EDNs including the seven from the Student search and also U-Net3+ as its combination with EfficientNetv2L and VGG-19 are available in the PyTorch framework. The results are shown in Table 3.

For both CNNs, the EDN of U-Net achieved the highest IoU and F1 scores. With VGG-19, three EDNs of U-Net, LinkNet, and U-Net++ achieved the highest average score (average of the four accuracy metrics) of 0.960 and an F1 of 0.967. Any of the three EDNs could serve well as the Teacher network. However, with EfficientNetv2L, only U-Net yielded the highest F1 score, marginally higher than DeepLabv3+, LinkNet, MANet, and U-Net++. FPN and PSPNet over-fit with VGG19 and FPN over-fit with EfficientNetv2L. U-Net3+ being the latest among the U-Net family, performed poorly with both CNNs. To choose

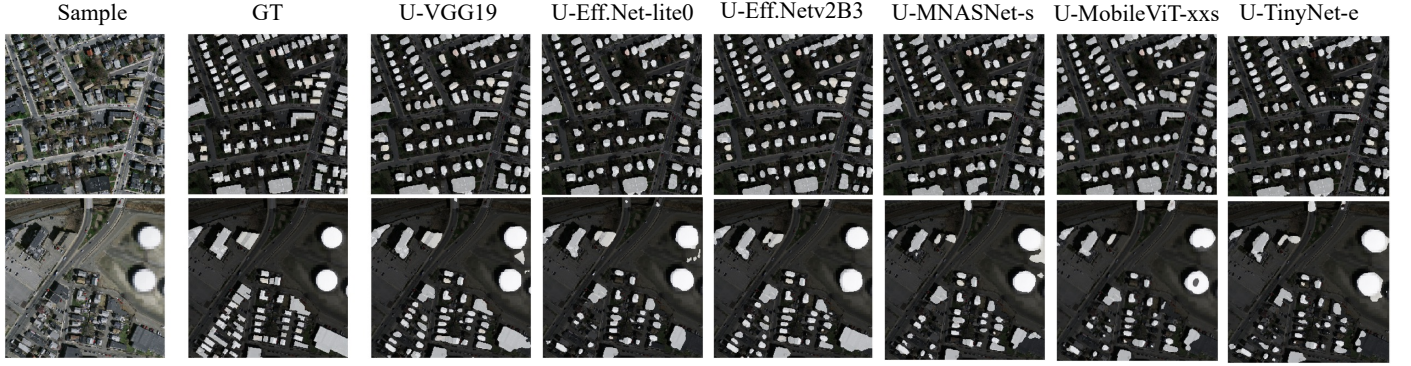


Figure 6: Segmentation performance of U-VGG19 and the selected Student networks on the subset of Massachusetts building dataset.

one Teacher network, U-Net with VGG-19 is taking the lead, despite marginal differences.

Table 3: Teacher search based on the highest-performing Student networks of U-EfficientNetv2B3 and U-VGG19. The highest and over-fitting scores are highlighted in bold and red respectively.

EDN	Par.	Loss	P	R	IoU	F1	ms/it
EDN with VGG19 encoder							
U-Net	29.1	0.033	0.959	0.976	0.938	0.967	226
DeepLabv3+	25.5	0.049	0.939	0.965	0.910	0.951	302
LinkNet	21.3	0.033	0.959	0.976	0.937	0.967	197
MANet	33.2	0.033	0.963	0.971	0.938	0.967	262
U-Net++	44.7	0.034	0.961	0.973	0.937	0.967	543
FPN	22.1	0.062	0.887	1.000	0.887	0.938	226
PSPNet	20.8	0.062	0.887	1.000	0.887	0.938	163
U-Net3+	24.8	0.049	0.934	0.970	0.910	0.951	610
EDN with EfficientNetv2L encoder							
U-Net	119.7	0.034	0.960	0.973	0.936	0.966	909
DeepLabv3+	117.7	0.036	0.956	0.975	0.934	0.965	840
LinkNet	117.1	0.035	0.955	0.976	0.934	0.965	990
MANet	130.7	0.035	0.958	0.973	0.935	0.965	935
U-Net++	120.7	0.035	0.955	0.977	0.935	0.965	990
FPN	118.3	0.062	0.887	1.000	0.887	0.938	971
PSPNet	116.5	0.041	0.948	0.971	0.924	0.959	275
U-Net3+	124.3	0.056	0.919	0.973	0.898	0.944	2001

Table 4: The baseline scores produced by the Teacher and Student networks without domain adaptation and distillation in the five settings of T-T, T-S, T-Ev, S-S, and S-Ev. These scores will be used as the baselines in the comparative study of the three knowledge transfer methods. The highest scores are highlighted in bold.

Network	Loss	P	R	IoU	F1	ms/it
Teacher evaluated on <i>val</i> of T (T-T)						
U-VGG19	0.080	0.929	0.917	0.860	0.920	235
Teacher evaluated on <i>val</i> of S (T-S)						
U-VGG19	0.186	0.770	0.894	0.713	0.814	40
Teacher evaluated on <i>val</i> of Ev (T-Ev)						
U-VGG19	0.169	0.877	0.814	0.746	0.831	40
Students trained on S and validated on S (S-S)						
U-VGG19	0.107	0.890	0.913	0.824	0.893	224
U-Eff.Net-lite0	0.155	0.838	0.877	0.754	0.845	190
U-Eff.Netv2B3	0.145	0.840	0.901	0.769	0.855	392
U-MNASNet-s	0.184	0.797	0.872	0.710	0.816	219
U-MobileViT-xxs	0.181	0.803	0.872	0.717	0.819	296
U-TinyNet-e	0.174	0.795	0.896	0.727	0.826	181
Student trained on S and validated on Ev (S-Ev)						
U-VGG19	0.215	0.866	0.741	0.676	0.785	41
U-Eff.Net-lite0	0.195	0.816	0.814	0.687	0.805	75
U-Eff.Netv2B3	0.181	0.838	0.819	0.708	0.819	96
U-MNASNet-s	0.235	0.784	0.773	0.639	0.765	56
U-MobileViT-xxs	0.233	0.814	0.748	0.634	0.767	154
U-TinyNet-e	0.221	0.808	0.776	0.648	0.779	56

3.4. Baseline Teacher and Students

The preliminary search of the hyperparameters, Teacher, and Student network brought forward the dice loss, RMSProp optimiser, six students (U-Net with VGG-19, EfficientNet-lite0, EfficientNetv2B3, MNASNet-s, MobileViT-xxs, and TinyNet-e) and one teacher of U-Net with VGG-19. The naming of the networks henceforth is done as U-VGG19 for U-Net with VGG-19, and similarly for other combinations. Next, we train them on the T and S datasets alone and produce the validation results on Ev to prepare the baseline scores for the experiments in the next sections. The results are shown in Table 4. The experiments are carried out in five settings of varying *train* and validation (*val*) data. T-T, T-S, and T-Ev are the settings with T, S, and Ev as the *val* data respectively and T as the train data in all settings. S-S and S-Ev settings represent the setting of training on S alone (without knowledge transfer), followed by validation on S and Ev respectively.

Teacher networks trained on T: The findings obtained from the T-T setting should be interpreted with caution due to the presence of unaccounted misalignment and noise in the samples of T. From the T-S setting, it is evident that the Teacher's ability to generalise the validation samples from S is influenced by the domain shift between T and S. This domain shift can be attributed to two primary factors: the presence of unfamiliar complex urban high-rise buildings in S and the contrast between precision of ortho-rectification between the samples of T and S. However, in the T-Ev setting, the Teacher demonstrates the capacity to generalise effectively to complex high-rise buildings in Ev, even though it was trained on misaligned labels. The complexity of the clean data S and Ev is visible in the experimental results.

Student networks trained alone on S: Among the six Student networks trained alone on S, U-VGG19 yields the highest F1 scores when validated on *val* of S, followed by U-EfficientNetv2B3 and U-EfficientNet-lite0. The same networks

when validated on Ev, U-EfficientNetv2B3 yield the highest IoU (0.708) and F1 score (0.819) making it the best Student network on Ev, when trained alone on S. This is for two reasons: (i) unlike U-NetVGG19, it allows model compression with the least degradation of performance when compared to the Teacher’s validation on Ev, and (ii) it also minimises the misalignment of labels.

With the baseline scores from this section, next, we show the performance of the Teacher and Student networks in the SDA, KD, and DML in order.

3.5. Supervised Domain Adaptation

SDA improved the performance of all Student networks when compared to the networks trained alone on S. The results are shown in Table 5 and can be compared to the networks of the same setting (S-S and S-Ev) from baseline Table 4. Here, the setting S-S represents the Student networks trained on T and further domain-adapted on S, and validated on the *val* set of S. S-Ev represents the same adapted networks validated on Ev. Compared to the baseline values of the same settings, all networks in both settings perform with higher scores on average. Specific to the F1 score, all networks in both settings, except U-EfficientNet-lite0 of the S-Ev setting outperform the baseline scores. All networks also outperform the Teacher (T-S setting from Table 4) on the *val* set of S. U-VGG19 and U-EfficientNetv2B3 yielded the highest scores in the settings of S-S (0.903 F1) and S-Ev (0.847 F1) respectively, suggesting the U-EfficientNetv2B3 to be the best Student network for SDA in the Ev dataset.

Table 5: SDA of the Student networks pre-trained on T and adapted on S. The scores of the corresponding settings are to be compared with the baseline scores from Table 4. The highest scores are highlighted in bold.

Network	Loss	P	R	IoU	F1	ms/it
SDA from T to S, and validated on S (S-S)						
U-VGG19	0.098	0.906	0.914	0.838	0.903	231
U-Eff.Net-lite0	0.138	0.859	0.890	0.778	0.862	194
U-Eff.Netv2B3	0.120	0.869	0.914	0.805	0.880	386
U-MNASNet-s	0.151	0.828	0.900	0.759	0.849	215
U-MobileViT-xxs	0.145	0.846	0.890	0.769	0.855	294
U-TinyNet-e	0.160	0.831	0.882	0.748	0.840	181
SDA from T to S, and validated on Ev (S-Ev)						
U-VGG19	0.173	0.917	0.784	0.737	0.827	48
U-Eff.Net-lite0	0.197	0.873	0.763	0.688	0.803	103
U-Eff.Netv2B3	0.153	0.874	0.837	0.752	0.847	95
U-MNASNet-s	0.205	0.844	0.772	0.690	0.795	55
U-MobileViT-xxs	0.191	0.848	0.793	0.694	0.809	149
U-TinyNet-e	0.222	0.844	0.741	0.653	0.779	56

3.6. Knowledge Distillation

KD is a model compression technique that is used to distil a Student network with lower network parameters from a Teacher network without significant loss in performance. Unlike the experiments of SDA, KD is performed between the Teacher network of U-VGG19 and the selected Student networks. Therefore, the difference between the number of parameters in the Teacher of U-VGG19 and that of Student networks is the number of reduced network parameters, except for U-VGG19 as a

Student network. The results are shown in Table 6. The S-S setting here represent the Student networks trained on T and further distilled on S, and validated on the *val* set of S. S-Ev represents the same distilled networks validated on Ev. Compared to the baseline values of the same settings from Table 4, most networks offer lower average evaluation scores and F1 scores. KD between the U-VGG19 shows better results in both S-S and S-Ev settings, but it does not offer model compression. U-MNASNet-s is the only exception that shows higher scores in the S-Ev setting. Among the smaller Students, U-EfficientNetv2B3 and U-EfficientNet-lite0 yielded the highest scores in the settings of S-S (0.851 F1) and S-Ev (0.784 F1) respectively, suggesting U-EfficientNet-lite0 to be the best Student network for KD in the Ev dataset with network parameters reduced by 82% from 29.1M (of U-VGG19) to 5.6M. The reduced number of parameters is shown in percentage in Table 6 and the network parameters were previously shown in Table 2.

Table 6: KD between the U-VGG19 Teacher trained on T and Student networks distilled on S. The scores of the corresponding settings are to be compared with the baseline scores from Table 4. The reduced network parameters from the Teacher of U-VGG19 are reported by Par. Red. column in percentage. The highest scores are highlighted in bold.

Network	Loss	P	R	IoU	F1	ms/it	Par. Red.
KD of Students from U-VGG19 (S-S)							
U-VGG19	0.099	0.907	0.895	0.820	0.901	410	0
U-Eff.Net-lite0	0.265	0.944	0.602	0.581	0.735	306	82
U-Eff.Netv2B3	0.149	0.895	0.810	0.740	0.851	467	50
U-MNASNet-s	0.199	0.869	0.744	0.669	0.801	278	93
U-MobileViT-xxs	0.214	0.811	0.763	0.648	0.786	346	89
U-TinyNet-e	0.179	0.860	0.785	0.696	0.821	315	92
Distilled Student validated on Ev (S-Ev)							
U-VGG19	0.184	0.877	0.772	0.707	0.812	40	0
U-Eff.Net-lite0	0.232	0.794	0.802	0.656	0.784	43	82
U-Eff.Netv2B3	0.219	0.844	0.735	0.650	0.774	77	50
U-MNASNet-s	0.223	0.756	0.842	0.654	0.781	52	93
U-MobileViT-xxs	0.320	0.840	0.610	0.538	0.688	93	89
U-TinyNet-e	0.294	0.826	0.638	0.554	0.702	46	92

3.7. Deep Mutual Learning

DML is another model compression technique that allows collaborative training of multiple Student networks. Similar to KD, the experiments are performed between the Teacher network of U-VGG19 and the selected Student networks. Only two Student networks are distilled at one time because of the computational costs associated with loading three EDNs (including one Teacher and two Students) into the GPU. We do not report the DML of U-MobileViT-xxs to keep the experiments short as it did not perform well in the previous experiments of KD. The results are shown in Table 7. The training and validation settings of S-S and S-Ev are the same as those of KD. The results can be explained in four categories:

- DML vs. Baseline (S-S): The performance of all networks is reduced compared to the baseline of the S-S setting.
- DML vs. Baseline (S-Ev): Comparing against the F1 scores of baselines, U-VGG19 improved when mutually trained with U-EfficientNetv2B3 and U-TinyNet-e. Similarly, U-TinyNet-e improved with U-VGG19

and U-EfficientNetv2B3, and U-MNASNet-s with U-EfficientNetv2B3. The combination of U-VGG19 and U-TinyNet-e improved them both in the same training. The other combinations did not yield a higher F1 score.

- DML vs. KD (S-S): Comparing against the F1 scores of KD, the majority of combinations yielded lower values, except U-MNASNet-s (with U-VGG19) and U-EfficientNet-lite0 (with U-EfficientNetv2B3).
- DML vs. KD (S-Ev): More Student networks improved on the Ev dataset. This includes U-EfficientNetv2B3 and U-TinyNet-e mutually trained with U-VGG19, and U-TinyNet-e and U-MNASNet-s with U-EfficientNetv2B3. The combination of U-EfficientNetv2B3 and U-MNASNet-s improved the F1 scores of both networks at the same time. If accounted for the average scores of the four metrics, the combination of U-VGG19 and U-TinyNet-e also improved both in the same training.

To summarise, DML improved the evaluation scores of many Student networks in the Ev dataset. However, this involved reducing the performance of at least one Student network for each combination. Only a few combinations such as U-VGG19 + U-TinyNet-e and U-EfficientNetv2B3 + U-MNASNet-s improved the score of each other. The combination of U-VGG19 + U-EfficientNetv2B3 yielded the highest scores on average in both S-S and S-Ev settings.

Table 7: DML between the U-VGG19 Teacher trained on T and two Student networks distilled on S. The scores of the corresponding settings are to be compared with the baseline scores from Table 4. The highest scores are highlighted in bold.

Network	Loss	P	R	IoU	F1	ms/it
DML of Students from U-VGG19 (S-S)						
U-VGG19	0.118	0.912	0.873	0.806	0.882	
U-Eff.Netv2B3	0.168	0.881	0.819	0.731	0.832	862
U-VGG19	0.121	0.913	0.869	0.802	0.879	
U-TinyNet-e	0.201	0.883	0.768	0.685	0.799	699
U-VGG19	0.117	0.907	0.882	0.808	0.883	
U-MNASNet-s	0.191	0.880	0.785	0.701	0.809	690
U-Eff.Netv2B3	0.172	0.879	0.817	0.726	0.828	
U-Eff.Net-lite0	0.179	0.886	0.798	0.717	0.821	775
U-Eff.Netv2B3	0.171	0.900	0.801	0.730	0.829	
U-TinyNet-e	0.196	0.881	0.776	0.693	0.804	840
U-Eff.Netv2B3	0.169	0.884	0.816	0.732	0.831	
U-MNASNet-s	0.203	0.884	0.763	0.684	0.797	800
DML of Students from U-VGG19 (S-Ev)						
U-VGG19	0.201	0.888	0.739	0.685	0.793	41
U-Eff.Netv2B3	0.192	0.829	0.810	0.696	0.810	78
U-VGG19	0.196	0.889	0.743	0.689	0.796	41
U-TinyNet-e	0.221	0.775	0.808	0.658	0.781	44
U-VGG19	0.204	0.883	0.731	0.678	0.784	47
U-MNASNet-s	0.253	0.805	0.722	0.615	0.748	50
U-Eff.Netv2B3	0.232	0.846	0.718	0.630	0.761	75
U-Eff.Net-lite0	0.254	0.611	0.999	0.610	0.746	47
U-Eff.Netv2B3	0.313	0.864	0.597	0.541	0.685	77
U-TinyNet-e	0.221	0.792	0.801	0.656	0.782	47
U-Eff.Netv2B3	0.210	0.845	0.747	0.658	0.782	76
U-MNASNet-s	0.218	0.767	0.838	0.665	0.790	50

4. Discussion

4.1. Summary from the results

Due to the large number of experiments, in this section, we summarise the results from the three knowledge transfer methods and compare the networks with the highest scores against the baselines. Figure 7 shows the summarised results, which report only the networks with the highest scores from the previous experiments. In the S-S setting, SDA outperforms the baseline scores and other methods with both U-VGG19 and U-EfficientNetv2B3. KD outperforms the baseline scores with U-VGG19. However, using U-VGG19 as the Student network does not offer model compression. With U-EfficientNetv2B3, there is a marginal degradation of scores with a reduction in 50% of network parameters (29.1M vs. 14.6M). Specifically in the F1 score, the degradation amounts to 0.004 (0.851 vs. 0.855) and 0.023 (0.832 vs. 0.855) in KD and DML respectively compared to the baseline. In the S-Ev setting, SDA outperforms the baseline scores and other methods with both U-VGG19 and U-EfficientNetv2B3. All three methods outperform the baseline scores with U-VGG19, without offering the model compression. With U-EfficientNetv2B3, the degradation of the F1 score amounts to 0.045 (0.774 vs. 0.819) and 0.009 (0.810 vs. 0.819) in KD and DML respectively against the baseline.

4.2. Effects of building heights and spatial resolution

The previous experiments reported the performance of SDA, KD, and DML against the baseline scores, with SDA as the best-performing method of knowledge transfer. Here, we separate the samples of the Ev dataset into four types of buildings: low-rise, mid-rise, high-rise, and skyscrapers. We report the performance of each method and compare them against the Teacher’s predictions as shown in Table 8. From the results, SDA outperforms the Teacher network on three low-rise, mid-rise, and skyscrapers. KD and DML are not able to outperform the Teacher network, making SDA the best-performing method to address the problem of misaligned labels. Both Student and Teacher networks yielded F1 and average scores above 0.9 for low-rise buildings. The performance degrades with the height of the buildings as seen from the results. For high-rise buildings, Teacher has shown the highest level of generalisation despite being trained on noisy data. The poorest results are obtained on the skyscrapers.

The results can be followed in Figure 8, which shows a sample result of each spatial resolution for the four building types. For the low-rise buildings, SDA has increased the generalisation of the buildings in all three resolutions and achieved the highest F1 score of 0.943. The green boxes highlight the network’s ability to individually segment the non-attached buildings. From the blue boxes in the 30cm image sample, it can be seen that the domain adapted and the distilled Student networks can separate the roofs from the facades. KD and DML over-segmented the images. As the building height increased to mid-rise, the evaluation scores visibly suffered. SDA once again shows improvement in the generalisation of the buildings. The blue boxes in the 60cm image sample show SDA’s ability

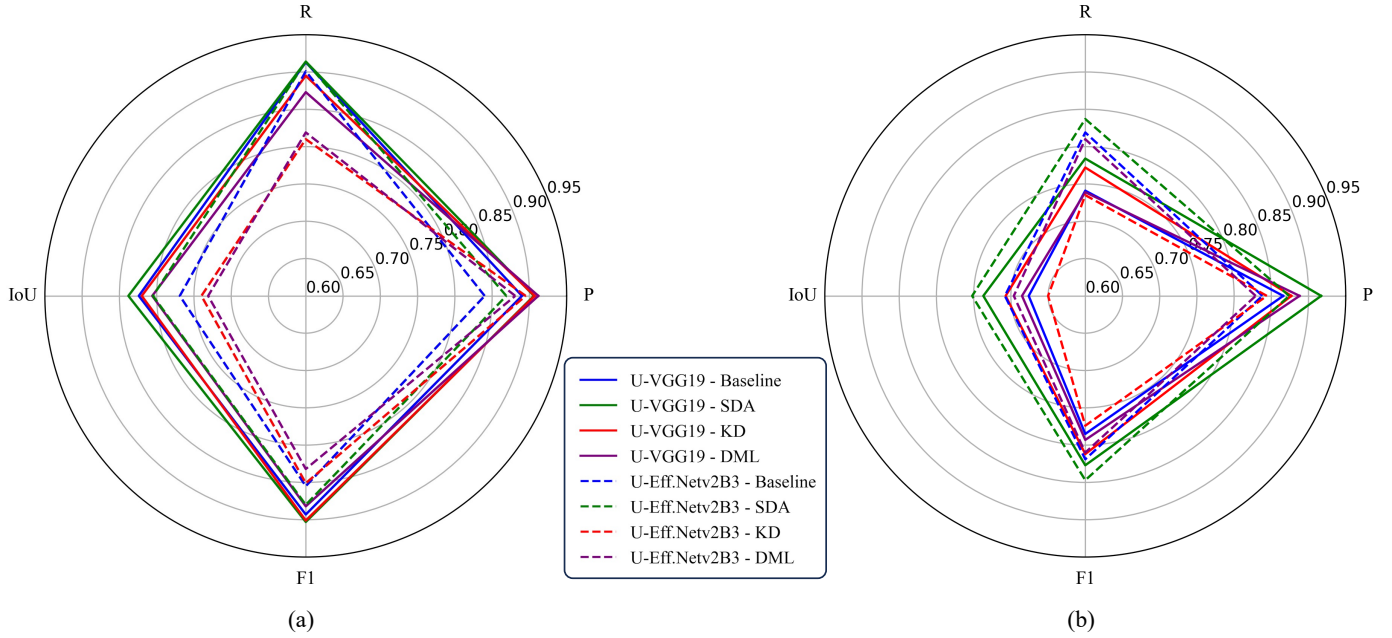


Figure 7: A spider chart to show the summary of results for U-VGG19 and U-EfficientNet2B3 Student networks adapted/distilled with U-VGG19 as Teacher in (a) S-S setting and (b) S-Ev setting. In the S-S setting, the SDA of U-VGG19 yielded the highest F1 score of 0.903, followed by KD (0.901 F1) with the same Student. In the S-Ev setting, the SDA of U-EfficientNet2B3 yielded the highest F1 score of 0.847, followed by the same network trained alone on S (baseline) with a 0.819 F1 score.

Table 8: Segmentation results of the Teacher, SDA, KD, and DML using U-VGG19 network on four types of buildings: low-rise, mid-rise, high-rise, and skyscrapers. The highest scores for each building type are highlighted in bold.

Buildings	Method	Network	P	R	IoU	F1	Avg.
Low-rise	Teacher		0.061	0.932	0.947	0.886	0.939
	SDA		0.057	0.943	0.942	0.893	0.943 0.930
	KD		0.071	0.945	0.920	0.874	0.932
	DML		0.073	0.952	0.907	0.868	0.928
Mid-rise	Teacher		0.133	0.880	0.858	0.772	0.867
	SDA		0.133	0.927	0.836	0.782	0.868 0.853
	KD		0.156	0.898	0.815	0.745	0.845
	DML		0.187	0.896	0.772	0.703	0.812
High-rise	Teacher		0.088	0.934	0.893	0.840	0.912 0.895
	SDA		0.132	0.962	0.794	0.773	0.868
	KD		0.146	0.948	0.764	0.730	0.842
	DML		0.186	0.954	0.686	0.665	0.792
Skyscrapers	Teacher		0.313	0.803	0.649	0.574	0.687
	SDA		0.303	0.870	0.630	0.575	0.697 0.693
	KD		0.308	0.777	0.638	0.545	0.686
	DML		0.318	0.800	0.618	0.540	0.677

to segment out the facades and the gaps between the buildings. For the high-rise, the Teacher network performs with the highest evaluation scores despite the noisy training data. However, from the samples, it is seen that SDA has shown better generalisation of roofs from the facades. The performance is the poorest for skyscrapers due to the shadows and complex roof structures. We highlight the skyscrapers with orange boxes in Figure 8 because of the lower resolution sample's large area coverage. Once again, SDA has produced the highest scores, but with increased noise. The 30cm sample in the Figure shows the segmentation of the tallest skyscraper in Melbourne with a height of 319m.

The spatial resolution of the images played different roles in the segmentation of the four building types. From the visual analysis, the adapted and distilled networks did not yield high scores in the highest resolution samples of 30cm. For low-rise, the size of the buildings was too small to accurately segment and for the high-rise and skyscrapers, the buildings were too large to fit into the image tiles, without providing global knowledge for the networks. The best visual results are produced on the resolution of 60cm, except for the skyscrapers. For skyscrapers, the lowest resolution of 120cm yielded visually best segmentation results.

4.3. The research questions

With the experimental summary and discussion, now we address the three research questions (**RQ1-3**) that this study sets out to answer. The preliminary study from our workflow of extensive comparative study answers the **RQ1** in a structured manner. Hyperparameters of dice loss, RMSProp optimiser, and 1e-4 learning rate yielded the highest evaluation scores on a U-Net EDN with MobileOne-s1 CNN. Jaccard loss and Adam optimisers were also marginally similar. Among the EDNs, U-Net++ with MobileOne-s1 encoder produced the highest scores in the subset benchmark dataset with up to 0.964 F1 score. Compared to U-Net++, U-Net provided the best trade-off between network parameters (9.1M vs. 12.3M) and evaluation scores with a marginally lower F1 score of 0.962 and less complexity in network architecture. Fewer parameters mean smaller model size and faster training time, which is essential for Student networks. With the best EDN found, 43 lightweight CNNs including low-latency networks from Google, Apple,

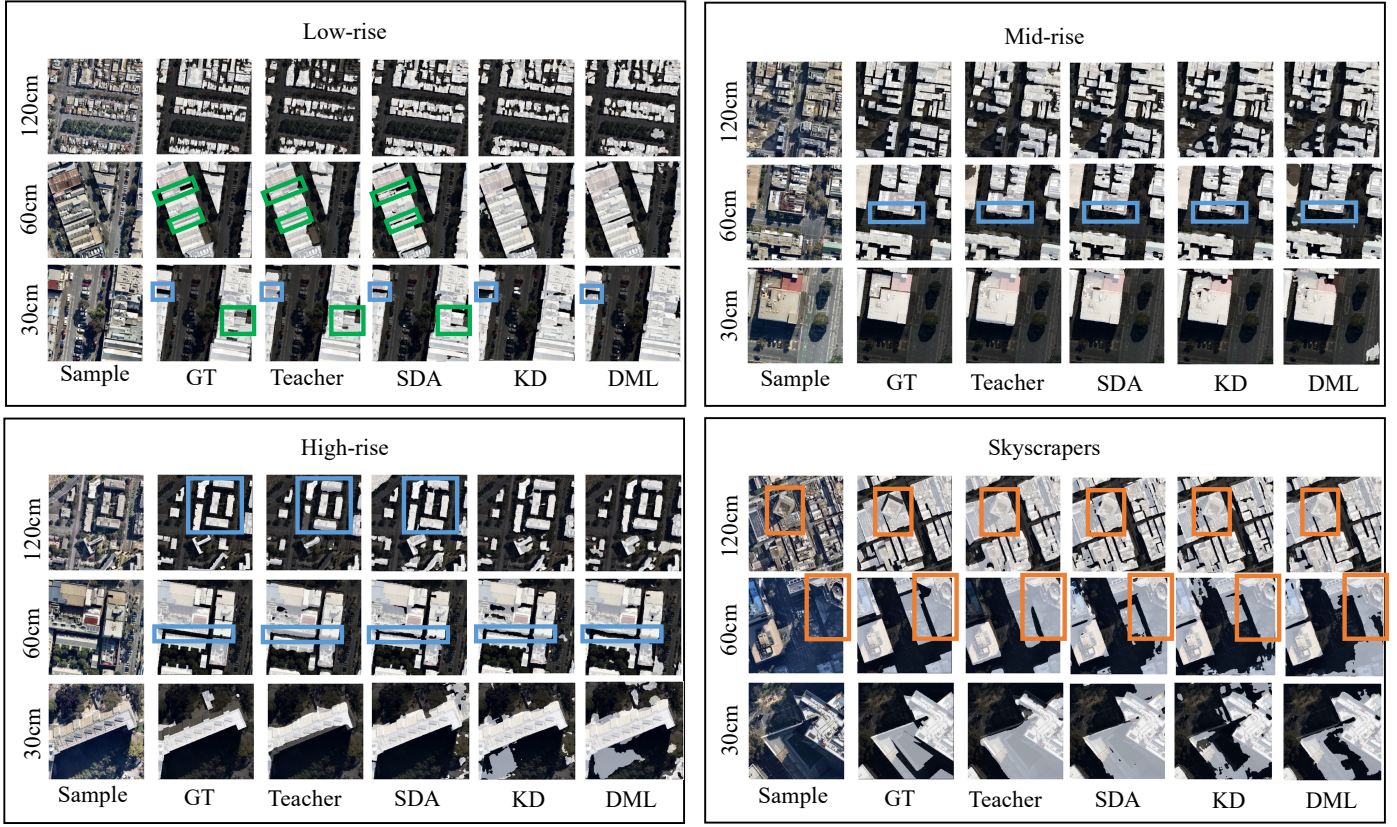


Figure 8: Result samples on four types of buildings and samples of different spatial resolutions. Green boxes highlight how the Student networks can separate the instances of separated buildings. The blue boxes show that the methods are trying not to detect the facades of the buildings. Orange boxes are used to highlight the skyscraper buildings in the provided samples. Each of the 30, 60, and 120cm samples shows skyscrapers of 177m, 251m, and 319m (the tallest building in Melbourne).

and Huawei were individually integrated into the U-Net architecture and benchmarked. EfficientNetv2B3 yielded the highest IoU of 0.934 and F1 of 0.965. EfficientNet-lite0 provided the best trade-off between the network parameters (5.6M) and evaluation scores (0.962 F1). MNASNet-s, TinyNet-e, and MobileViT-xxs produced the lightest U-Net architectures with 2.2, 2.3, and 3.1M parameters. These five CNNs in the U-Net EDN serve as the best Students for efficiency gain. With the EfficientNetv2B3 as the highest-scoring Student, the largest version of the same family, EfficientNetv2L, is selected as the CNN for the Teacher along with VGG-19 which produced the highest scores in our previous benchmarks. Among eight EDNs, U-Net yielded the highest scores with both VGG-19 (0.967 F1) and EfficientNetv2L (0.966 F1). To choose one, U-Net with VGG-19 (U-VGG19) is the top-scoring Teacher network for KD and DML.

Finding the best Teacher and Students allowed fair comparison among SDA and model compression techniques of KD and DML to answer **RQ2**. Looking for the high scorers from SDA, KD, and DML on the Ev dataset, U-EfficientNetv2B3 is the best Student network for SDA but without model compression. KD and DML offered compression, with a small loss in evaluation scores. U-EfficientNet-lite0 is the best Student for KD with an 82% reduction in network parameter (from 29.1M to 5.6M) from the Teacher of U-VGG19. Only a few

combinations of Students improved the scores of both Students when trained in the collaborative manner of DML. Two Student pairs of (U-VGG19, U-TinyNet-e) and (U-EfficientNetv2B3, U-MNASNet-s) increased the F1 scores of both Students at the same training, compared to the baseline (networks without distillation) and KD respectively. Therefore, SDA provided the highest evaluation scores, KD was efficient in model compression, and DML successfully allowed collaborative learning among Student pairs to improve each other's performance. However, SDA was more successful in minimising the effects of misaligned building labels.

Answering the **RQ3**, SDA, KD, and DML perform differently on varying building heights and spatial resolutions of EO images. Specific to the building heights, SDA yielded the highest scores of up to on low-rise (0.943 F1), mid-rise (0.868 F1), and skyscrapers (0.697 F1), suggesting it to be the best knowledge transfer method to minimise the effects of misaligned building labels in most building types. Despite being trained on the misaligned labels, the Teacher network still generalised the high-rise buildings with the highest F1 score of 0.912. KD and DML are not able to outperform the Teacher networks, and the poorest results are obtained on skyscrapers. All three knowledge transfer methods reduced the segmentation of facades and the gaps among the nearby buildings. Talking about spatial resolution, SDA increased the generalisation of the buildings in

the aerial images of all three spatial resolutions of 30, 60, and 120cm. The resolution of 60cm produced the best qualitative results, except for the skyscrapers. Because of the large area coverage of the skyscrapers, the best visual results are obtained from the resolution of 120cm. Precise segmentation is not produced on the highest resolution of 30cm.

5. Conclusion

This study presented a structured workflow to compare three knowledge transfer methods to tackle the problem of misaligned building labels due to off-nadir EO imagery. The three methods – SDA, KD, and DML – were recently introduced for the problem but lacked a study under different influences of DL configurations, building height, and spatial resolution of EO imagery. Our comparison fills this gap by answering three key questions that are listed at the beginning of the paper. Additionally, a set of building footprint datasets with pixel-level large-noisy and small-clean training datasets was unavailable to study these methods. We developed the required datasets inclusive of four building types and images of three spatial resolutions.

Our structured comparison begins with a preliminary study of finding the best hyperparameters, Teachers, and Students for the three knowledge transfer methods. This step allowed the construction of EDN configurations with the highest evaluation scores to be selected as Teachers and Students. Secondly, three datasets (T, S, and Ev) were developed to train and evaluate the identified best Teachers and Students. T contains misaligned image-label pairs, S contains a combination of misaligned and orthorectified images with manually annotated precise labels for complex urban buildings, and Ev contains misaligned image subsets from T with manually annotated precise labels. Ev is the main dataset that is used to validate the knowledge transfer methods. Finally, the performance of SDA, KD, and DML were studied on four building types with varying heights, and three spatial resolution of EO images. The three methods allowed two-step training of noise-tolerant EDNs in a Teacher-Student setting to minimise the effects of misalignment of building labels in the training data.

The preliminary study of the comparison identified that the best hyperparameters to train an EDN (constructed with randomly selected MobileOne-s1 CNN from Apple and a U-Net EDN) were: RMSProp as an optimiser and Dice loss as a loss function that yielded up to 0.962 F1 with least loss of 0.039. With the best hyperparameters identified, several lightweight CNNs from leading tech industries like Google, Apple, Facebook, and Huawei were studied as potential Student networks. Google's EfficientNetv2B3 CNN with U-Net EDN (0.965 F1) served as the best Student with the highest evaluation scores. Similarly, U-EfficientNet-lite0 (0.962 F1) provided the best trade-off between the scores, network parameters, and the time taken to train the network. Among the three knowledge transfer methods, SDA was the most effective method to address the misalignment problem. It was robust for all building types with the highest F1 scores in low-rise (0.943), mid-rise (0.868), high-rise (0.912), and skyscrapers (0.697). The model compression methods of KD and DML were less effective than SDA in

addressing the problem but were able to compress the DL networks up to 82% without performance loss.

In the broader spectrum of EO and building extraction, the results concluded that building height and spatial resolution of EO images strongly affect the precision of semantic segmentation for all three knowledge transfer methods. The experiments show that 60cm spatial resolution provides the best trade-off between local and global context information for low-rise, mid-rise, and high-rise buildings. However, a lower resolution of 120cm produced the best qualitative results in the segmentation of skyscrapers, as the footprints of the buildings are larger. This concludes that the spatial resolution is important depending on the footprint of the buildings, which rises with the building height.

With 158 experiments, we have successfully answered the three RQs that remained unanswered before this study. The answers and the multiple findings of this study will be crucial to future studies of EO-based urban feature extraction. Further, the developed datasets will be valuable in addressing the problem of misaligned building labels due to off-nadir images. The future direction of the study will be in the improvement of the datasets with additional classes such as "building facades" and refinement of DML techniques with a diverse loss function between multiple Students. This will facilitate precise urban feature extraction and progressive digital twin technologies.

Acknowledgement

The first author (B.N.) is supported by the University of Melbourne for his Ph.D. research and has been awarded by Melbourne Research Scholarship. The authors would like to thank Nearmap for providing the API service to collect the image data for the experiments. The authors also express their special gratitude to *Segmentation Models Pytorch* and *Hugging Face* for their continuous support towards open and accessible AI – the extensive study would not have been possible without their commendable work.

References

- [1] T. Bakirman, I. Komurcu, E. Sertel, Comparative analysis of deep learning based building extraction methods with the new vhr istanbul dataset, *Expert Systems with Applications* 202 (2022) 117346.
- [2] B. Neupane, J. Aryal, A. Rajabifard, Rethinking the u-net, resunet, and u-net3+ architectures with dual skip connections for building footprint extraction (2023). [arXiv:2303.09064](https://arxiv.org/abs/2303.09064).
- [3] G. Xu, M. Deng, G. Sun, Y. Guo, J. Chen, Improving building extraction by using knowledge distillation to reduce the impact of label noise, *Remote Sensing* 14 (22) (2022) 5645.
- [4] B. Neupane, J. Aryal, A. Rajabifard, Building footprint segmentation using transfer learning: a case study of the city of melbourne, *ISPRS Annals of the Photogrammetry, Remote Sensing and Spatial Information Sciences* 10 (2022) 173 – 179. doi:10.5194/isprs-annals-X-4-W3-2022-173-2022.
- [5] G. Hinton, O. Vinyals, J. Dean, et al., Distilling the knowledge in a neural network, *arXiv preprint arXiv:1503.02531* 2 (7) (2015).
- [6] Y. Zhang, T. Xiang, T. M. Hospedales, H. Lu, Deep mutual learning, in: *Proceedings of the IEEE conference on computer vision and pattern recognition*, 2018, pp. 4320–4328.

- [7] L. Wang, S. Fang, X. Meng, R. Li, Building extraction with vision transformer, *IEEE Transactions on Geoscience and Remote Sensing* 60 (2022) 1–11.
- [8] K. He, X. Zhang, S. Ren, J. Sun, Deep residual learning for image recognition, in: *Proceedings of the IEEE conference on computer vision and pattern recognition*, 2016, pp. 770–778.
- [9] K. Simonyan, A. Zisserman, Very deep convolutional networks for large-scale image recognition, *arXiv preprint arXiv:1409.1556* (2014).
- [10] G. Huang, Z. Liu, L. Van Der Maaten, K. Q. Weinberger, Densely connected convolutional networks, in: *Proceedings of the IEEE conference on computer vision and pattern recognition*, 2017, pp. 4700–4708.
- [11] S. Saito, T. Yamashita, Y. Aoki, Multiple object extraction from aerial imagery with convolutional neural networks, *Electronic Imaging* 2016 (10) (2016) 1–9.
- [12] J. Long, E. Shelhamer, T. Darrell, Fully convolutional networks for semantic segmentation, in: *Proceedings of the IEEE conference on computer vision and pattern recognition*, 2015, pp. 3431–3440.
- [13] O. Ronneberger, P. Fischer, T. Brox, U-net: Convolutional networks for biomedical image segmentation, in: *International Conference on Medical image computing and computer-assisted intervention*, Springer, 2015, pp. 234–241.
- [14] Z. Zhang, Q. Liu, Y. Wang, Road extraction by deep residual u-net, *IEEE Geoscience and Remote Sensing Letters* 15 (5) (2018) 749–753. doi: 10.1109/LGRS.2018.2802944.
- [15] Z. Zhou, M. M. R. Siddiquee, N. Tajbakhsh, J. Liang, Unet++: Redesigning skip connections to exploit multiscale features in image segmentation, *IEEE transactions on medical imaging* 39 (6) (2019) 1856–1867.
- [16] H. Huang, L. Lin, R. Tong, H. Hu, Q. Zhang, Y. Iwamoto, X. Han, Y.-W. Chen, J. Wu, Unet 3+: A full-scale connected unet for medical image segmentation, in: *ICASSP 2020-2020 IEEE International Conference on Acoustics, Speech and Signal Processing (ICASSP)*, IEEE, 2020, pp. 1055–1059.
- [17] A. Chaurasia, E. Culurciello, Linknet: Exploiting encoder representations for efficient semantic segmentation, in: *2017 IEEE visual communications and image processing (VCIP)*, IEEE, 2017, pp. 1–4.
- [18] H. Zhao, J. Shi, X. Qi, X. Wang, J. Jia, Pyramid scene parsing network, in: *Proceedings of the IEEE conference on computer vision and pattern recognition*, 2017, pp. 2881–2890.
- [19] T.-Y. Lin, P. Dollár, R. Girshick, K. He, B. Hariharan, S. Belongie, Feature pyramid networks for object detection, in: *Proceedings of the IEEE conference on computer vision and pattern recognition*, 2017, pp. 2117–2125.
- [20] L.-C. Chen, Y. Zhu, G. Papandreou, F. Schroff, H. Adam, Encoder-decoder with atrous separable convolution for semantic image segmentation, in: *Proceedings of the European conference on computer vision (ECCV)*, 2018, pp. 801–818.
- [21] T. Fan, G. Wang, Y. Li, H. Wang, Ma-net: A multi-scale attention network for liver and tumor segmentation, *IEEE Access* 8 (2020) 179656–179665.
- [22] J. Yuan, Learning building extraction in aerial scenes with convolutional networks, *IEEE transactions on pattern analysis and machine intelligence* 40 (11) (2017) 2793–2798.
- [23] V. Mnih, G. E. Hinton, Learning to label aerial images from noisy data, in: *Proceedings of the 29th International conference on machine learning (ICML-12)*, 2012, pp. 567–574.
- [24] T. Xiao, T. Xia, Y. Yang, C. Huang, X. Wang, Learning from massive noisy labeled data for image classification, in: *Proceedings of the IEEE conference on computer vision and pattern recognition*, 2015, pp. 2691–2699.
- [25] S. Sukhbaatar, J. Bruna, M. Paluri, L. Bourdev, R. Fergus, Training convolutional networks with noisy labels, *arXiv preprint arXiv:1406.2080* (2014).
- [26] J. Goldberger, E. Ben-Reuven, Training deep neural-networks using a noise adaptation layer, in: *International conference on learning representations*, 2016.
- [27] E. Maggiori, Y. Tarabalka, G. Charpiat, P. Alliez, Convolutional neural networks for large-scale remote-sensing image classification, *IEEE Transactions on geoscience and remote sensing* 55 (2) (2016) 645–657.
- [28] V. Mnih, Machine learning for aerial image labeling, Ph.D. thesis, University of Toronto, accessed on: 12-06-2023 (2013).
URL https://www.cs.toronto.edu/~vmnih/docs/Mnih_Volodymyr_PhD_Thesis.pdf
- [29] S. Ji, S. Wei, M. Lu, A scale robust convolutional neural network for automatic building extraction from aerial and satellite imagery, *International journal of remote sensing* 40 (9) (2019) 3308–3322.
- [30] E. Maggiori, Y. Tarabalka, G. Charpiat, P. Alliez, Can semantic labeling methods generalize to any city? the inria aerial image labeling benchmark, in: *2017 IEEE International Geoscience and Remote Sensing Symposium (IGARSS)*, IEEE, 2017, pp. 3226–3229.
- [31] Q. Chen, L. Wang, Y. Wu, G. Wu, Z. Guo, S. L. Waslander, Aerial imagery for roof segmentation: A large-scale dataset towards automatic mapping of buildings, *ISPRS Journal of Photogrammetry and Remote Sensing* 147 (2019) 42–55.
- [32] R. Gupta, R. Hosfelt, S. Sajeev, N. Patel, B. Goodman, J. Doshi, E. Heim, H. Choset, M. Gaston, xbd: A dataset for assessing building damage from satellite imagery, *arXiv preprint arXiv:1911.09296* (2019).
- [33] W. Li, C. He, J. Fang, J. Zheng, H. Fu, L. Yu, Semantic segmentation-based building footprint extraction using very high-resolution satellite images and multi-source gis data, *Remote Sensing* 11 (4) (2019) 403.
- [34] P. K. A. Vasu, J. Gabriel, J. Zhu, O. Tuzel, A. Ranjan, Mobileone: An improved one millisecond mobile backbone, in: *Proceedings of the IEEE/CVF Conference on Computer Vision and Pattern Recognition*, 2023, pp. 7907–7917.
- [35] M. Tan, Q. Le, Efficientnetv2: Smaller models and faster training, in: *International conference on machine learning*, PMLR, 2021, pp. 10096–10106.
- [36] B. Wu, X. Dai, P. Zhang, Y. Wang, F. Sun, Y. Wu, Y. Tian, P. Vajda, Y. Jia, K. Keutzer, Fbnnet: Hardware-aware efficient convnet design via differentiable neural architecture search, in: *Proceedings of the IEEE/CVF conference on computer vision and pattern recognition*, 2019, pp. 10734–10742.
- [37] S. Mehta, M. Rastegari, Mobilevit: light-weight, general-purpose, and mobile-friendly vision transformer, *arXiv preprint arXiv:2110.02178* (2021).
- [38] M. Tan, B. Chen, R. Pang, V. Vasudevan, M. Sandler, A. Howard, Q. V. Le, Mnasnet: Platform-aware neural architecture search for mobile, in: *Proceedings of the IEEE/CVF conference on computer vision and pattern recognition*, 2019, pp. 2820–2828.
- [39] K. Han, Y. Wang, Q. Zhang, W. Zhang, C. Xu, T. Zhang, Model rubik's cube: Twisting resolution, depth and width for tinynets, *Advances in Neural Information Processing Systems* 33 (2020) 19353–19364.
- [40] B. Neupane, J. Aryal, A. Rajabifard, Cnns for remote extraction of urban features: A survey-driven benchmarking, Available at SSRN 4537529 Accessed on: 05-09-2023 (2022).
- [41] A. G. Howard, M. Zhu, B. Chen, D. Kalenichenko, W. Wang, T. Weyand, M. Andreetto, H. Adam, Mobilenets: Efficient convolutional neural networks for mobile vision applications, *arXiv preprint arXiv:1704.04861* (2017).
- [42] M. Sandler, A. Howard, M. Zhu, A. Zhmoginov, L.-C. Chen, Mobilenetv2: Inverted residuals and linear bottlenecks, in: *Proceedings of the IEEE conference on computer vision and pattern recognition*, 2018, pp. 4510–4520.
- [43] A. Howard, M. Sandler, G. Chu, L.-C. Chen, B. Chen, M. Tan, W. Wang, Y. Zhu, R. Pang, V. Vasudevan, et al., Searching for mobilenetv3, in: *Proceedings of the IEEE/CVF international conference on computer vision*, 2019, pp. 1314–1324.
- [44] B. Zoph, Q. V. Le, Neural architecture search with reinforcement learning, *arXiv preprint arXiv:1611.01578* (2016).
- [45] M. Tan, Q. Le, Efficientnet: Rethinking model scaling for convolutional neural networks, in: *International conference on machine learning*, PMLR, 2019, pp. 6105–6114.
- [46] X. Li, W. Wang, X. Hu, J. Yang, Selective kernel networks, in: *Proceedings of the IEEE/CVF conference on computer vision and pattern recognition*, 2019, pp. 510–519.
- [47] Y. Chen, J. Li, H. Xiao, X. Jin, S. Yan, J. Feng, Dual path networks, *Advances in neural information processing systems* 30 (2017).
- [48] H. Zhang, C. Wu, Z. Zhang, Y. Zhu, H. Lin, Z. Zhang, Y. Sun, T. He, J. Mueller, R. Manmatha, et al., Resnest: Split-attention networks, in: *Proceedings of the IEEE/CVF Conference on Computer Vision and Pattern Recognition*, 2022, pp. 2736–2746.
- [49] M. Lin, H. Chen, X. Sun, Q. Qian, H. Li, R. Jin, Neural architecture design for gpu-efficient networks, *arXiv preprint arXiv:2006.14090* (2020).
- [50] J. Wang, K. Sun, T. Cheng, B. Jiang, C. Deng, Y. Zhao, D. Liu, Y. Mu,

- M. Tan, X. Wang, et al., Deep high-resolution representation learning for visual recognition, *IEEE transactions on pattern analysis and machine intelligence* 43 (10) (2020) 3349–3364.
- [51] N. Nayman, Y. Aflalo, A. Noy, L. Zelnik, Hardcore-nas: Hard constrained differentiable neural architecture search, in: International Conference on Machine Learning, PMLR, 2021, pp. 7979–7990.
- [52] M. Tan, Q. V. Le, Mixconv: Mixed depthwise convolutional kernels, in: 30th British Machine Vision Conference 2019, BMVC 2019, Cardiff, UK, September 9-12, 2019, BMVA Press, 2019, p. 74.
URL <https://bmvc2019.org/wp-content/uploads/papers/0583\-\paper.pdf>
- [53] A. Saha, P. Rai, H. Daumé, S. Venkatasubramanian, S. L. DuVall, Active supervised domain adaptation, in: Joint European Conference on Machine Learning and Knowledge Discovery in Databases, Springer, 2011, pp. 97–112.
- [54] J. Yosinski, J. Clune, Y. Bengio, H. Lipson, How transferable are features in deep neural networks?, *Advances in neural information processing systems* 27 (2014).
- [55] P. Iakubovskii, Segmentation models pytorch, accessed on 22-07-2023 (2019).
URL https://github.com/qubvel/segmentation_models.pytorch